Modular Response in Free Quantum Fields:
A KMS/FDT Theorem and Conditional Extensions

[clg][1]

[1][Institutions]
(Dated:)

Part I (Theoremic core, free/Gaussian Hadamard QFT). We prove that, for small causal diamonds (CHM) in locally Hadamard states and within a safe window $\epsilon_{\mathrm{UV}} \ll \ell \ll \min\{L_{\mathrm{curv}}, \lambda_{\mathrm{mfp}}, m_i^{-1}\}$, the MI/moment-kill projector isolates a finite ℓ^4 modular response with coefficient equal to its flat-space value; the projected KMS/FDT susceptibility is positive; and coarse-graining over the wedge family produces the universal weak-field prefactor $5/12 = (4/3) \times (5/16)$. The fractional KMS defect between CHM diamonds and half-spaces scales as $\mathcal{O}((\ell/L_{\mathrm{curv}})^2) + \mathcal{O}((\ell H)^2)$. The QFT sensitivity is $\beta = 2\pi C_T I_{00} = 0.02086 \pm 0.00105$ (conservative 5% shared systematics from four independent routes). A scheme-invariant background relation *suggests* $\Omega_\Lambda = \beta\, f\, c_{\mathrm{geo}}$ *conditional* on our coarse-graining and analyticity assumptions.

Part II (Conditional extensions). We separate *definition* (flat-space ε from modular response) from *mapping*. Rather than impose the standard EFT-of-DE α-basis, we adopt a quasi-static closure that keeps operational distances GR-like (no additional lensing coupling $\Sigma \simeq 1$) while modifying growth via $\mu(\varepsilon_{\mathrm{eff}}, s) = 1/(1 + \frac{5}{12}\varepsilon_{\mathrm{eff}}\, s(x))$ with $s(x)$ a local, covariant environment modulation derived from the action and $\varepsilon_{\mathrm{eff}}$ a *species-gated* state variable (Sec. IV). KMS/FDT positivity motivates an entropy-driven law $d\bar\varepsilon/d\ln a \geq 0$ with a *conditional* background budget $\int \bar\varepsilon\, d\ln a = \Omega_\Lambda$ using species-aware safe-window fractions $f_V^{(i)}$ (Sec. IV). Cosmological illustrations (S_8 band and H_0 bounds) are **toy/illustrative** and propagate the $\pm 5\%$ β uncertainty; *observed lensing amplitudes still reflect the altered growth.*

Part III (Exploratory). (i) An *optional*, shock-selective *optical* channel (Assumption D$'$) reduces Σ only in high-shear shocked gas to address Bullet-type lensing offsets while preserving FRW distances. We retain a simple local saturating law in the text, and now provide a *principled derivation path* from Schwinger–Keldysh (SK) hydrodynamics that makes α_{opt} a calculable function of ICM transport coefficients (App. XXIV; App. XXV). (ii) A compact thermodynamic interpretation of the projected modular response: a Clausius-like identity holds at working order in the MI/moment-kill channel, and the FRW budget may be viewed as a *coarse-grained* Clausius normalization *conditional* on our KMS→FRW hypotheses. We clarify the relation to the Casini–Galante–Myers critique of Jacobson.

READER'S MAP: PART I (THEOREM) VS. PART II (CONDITIONAL) VS. PART III (EXPLORATORY)

Part I (Secs. I–V, Apps. XVI–XIX): proven results for free/Gaussian Hadamard fields at working order, plus SM bookkeeping and f_V linkage (Sec. IV).
Part II (Secs. VI–XXVI, Apps. XX–XXI, XXII): conditional extensions, Assumptions C & D (stated), safe-window fraction, KMS→FRW link, *action-derived* environment modulation, entropic sketch, and toy/illustrative numerics with propagated uncertainties.
Part III (Secs. VIII C, XIV, Apps. XXIV, XXV): exploratory shock-selective optical response (Assumption D$'$) with an SK/BRSSS derivation path and a thermodynamic interpretation (Clausius form in the projected channel; conditional FRW budget) and relation to CGM's critique of Jacobson.

I. SCOPE, WORKING ORDER, AND SAFE-WINDOW QUANTIFICATION (PART I)

a. Working order and state class. We work to $\mathcal{O}(\ell^4)$ in the MI/moment-kill projector channel, treating curvature/contact terms as $\mathcal{O}(\ell^6)$. States are locally Hadamard.
b. KMS applicability (CHM diamonds). Exact BW KMS holds for half-spaces; CHM diamonds inherit it with fractional defect $\mathcal{O}((\ell/L_{\mathrm{curv}})^2) + \mathcal{O}((\ell H)^2)$ (App. XIX).
c. Safe-window volume fraction. Define a conservative admissible scale

$$\ell_{\max}(x) \equiv \zeta\, \min\left\{ L_{\mathrm{curv}}(x),\ \lambda_{\mathrm{mfp}}(x),\ m_i^{-1}(x) \right\}, \qquad \zeta = 0.1. \tag{1}$$

Using Press–Schechter/Sheth–Tormen mass functions and NFW curvature proxies $L_{\mathrm{curv}}^{-2} \sim (R_{abcd}R^{abcd})^{1/2}$ with substructure excision parameter ξ, we estimate the comoving volume fraction $f_V(\ell_{\min}) = \mathrm{Vol}\{x : \ell_{\max}(x) > \ell_{\min}\}/\mathrm{Vol}_{\mathrm{tot}}$.

A semi-analytic survey (App. XX) shows voids dominate f_V, while dense cores lack a window; representative values at $z \sim 0$ for $\ell_{\min} \in [1, 100]$ pc are $f_V \sim 0.6-0.95$ for $\xi \in [0.2, 0.5]$. This enters only as a domain-of-validity indicator.

   d. Spectrum caveat and GR reversion. The admissible window $\epsilon_{\mathrm{UV}} \ll \ell \ll \min\{L_{\mathrm{curv}}, \lambda_{\mathrm{mfp}}, m_i^{-1}\}$ is understood to apply to sectors that contribute at working order. Massive sectors with $\ell \gg m_i^{-1}$ are exponentially suppressed and, after MI/moment–kill subtraction, do not re-introduce lower moments or $\ell^4 \log \ell$ terms. Thus the ℓ^4 coefficient is dominated by massless/light fields while heavy fields decouple in this channel. When *all* contributing sectors are gated out or when curvature drives $s(x) \to 0$, the effective coupling reverts to GR, $\mu \to 1$ (Sec. IV).

   e. Angle invariance as a null test. The continuous-angle product $\mathcal{C}_\Omega = f(\theta) \, c_{\mathrm{geo}}(\theta)$ is analytic and θ-independent; residuals are shown as a null check, not a precision claim.

II. A2–KMS THEOREM (GAUSSIAN/HADAMARD SECTOR)

Theorem 1 (Projected modular response and positivity)**.** *Let $\mathcal{Q}$ be a free (Gaussian) QFT on a globally hyperbolic spacetime and ρ a locally Hadamard state. For a causal diamond of radius ℓ with $\ell \ll L_{\mathrm{curv}}$ and the MI/moment-kill projector that cancels r^0 and r^2 moments, the MI-subtracted modular response obeys*

$$\delta\langle K_{\mathrm{sub}} \rangle = (2\pi C_T I_{00}) \, \ell^4 \, \delta\varepsilon + \mathcal{O}(\ell^6), \tag{2}$$

with coefficient equal to the flat-space value. The retarded susceptibility χ_{QK} in the projected channel is positive (FDT), and wedge averaging yields the universal weak-field prefactor $5/12$. The fractional deviation from BW KMS is $\mathcal{O}((\ell/L_{\mathrm{curv}})^2) + \mathcal{O}((\ell H)^2)$.

Corollary 1 (Conditional background statement)**.** *Under the coarse-graining and analyticity assumptions of Sec. VII, the FRW zero mode* suggests *the scheme-invariant relation $\Omega_\Lambda = \beta \, f \, c_{\mathrm{geo}}$ with $\beta = 2\pi C_T I_{00}$. We treat this as a conditional statement rather than a theorem.*

III. QFT INPUT: $\beta = 2\pi C_T I_{00}$ AND ERROR BUDGET

   We evaluate β via four independent routes: (a) real-space CHM; (b) spectral/Bessel; (c) Euclidean time-slicing; (d) replica finite-difference. The spread is $\lesssim 1\%$. We adopt a conservative

$$\beta = 0.02086 \pm 0.00105 \quad (5\% \text{ shared systematics}). \tag{3}$$

Angle invariance is used as a null residual test.
Here C_T denotes the flat-space stress-tensor two-point normalization, e.g. $\langle T_{ab}(x) \, T_{cd}(0) \rangle = C_T \, \mathcal{I}_{abcd}(x)/|x|^{2d}$ in d dimensions (see Osborn–Petkou).
Benchmark (convention). For a free, massless real scalar in $d = 4$ and our normalization, $C_T = 1/(120\pi^2)$, which yields $\beta \simeq 0.02086$ via Eq. (7).
Implementation consistency (note). The normative constants used for the numerical reproductions are

$$C_T = \frac{1}{120\pi^2}, \qquad (\sigma_1, \sigma_2) = \left(\tfrac{1}{2}, 2\right), \qquad (a, b) = \left(\tfrac{4}{5}, \tfrac{1}{5}\right),$$

with the moment-kill identities enforced exactly (App. XVI). Helper scripts (`beta_methods_v2.py`, `referee_pipeline.py`) print these values alongside the computed I_{00} to prevent normalization drift.[1]
Reproducibility (non-circular). We use a two–scale MI/moment-kill subtraction with a top-hat window on 3-balls

$$W_\ell(r) = \frac{3}{4\pi\ell^3} \, \Theta(\ell - r), \qquad \mathcal{W}_\ell := \int_{B_\ell} W_\ell - a \int_{B_{\sigma_1 \ell}} W_{\sigma_1 \ell} - b \int_{B_{\sigma_2 \ell}} W_{\sigma_2 \ell}.$$

The two moment-kill conditions (cancelling r^0 and r^2 for any smooth radial F) fix

$$a + b = 1, \qquad a \, \sigma_1^2 + b \, \sigma_2^2 = 1 \implies a = \frac{\sigma_2^2 - 1}{\sigma_2^2 - \sigma_1^2}, \quad b = \frac{1 - \sigma_1^2}{\sigma_2^2 - \sigma_1^2}.$$

---

[1] In earlier development branches some convenience flags defaulted to alternate normalizations (e.g. $C_T = 3/\pi^4$) and near-unity MI scales. These have been disabled in the archival runners; the paper's conventions are authoritative.

In our runs we take

$$(\sigma_1, \sigma_2) = \left(\tfrac{1}{2}, 2\right), \qquad (a, b) = \left(\tfrac{4}{5}, \tfrac{1}{5}\right) = (0.8, 0.2).$$

With these weights the projected ℓ^4 coefficient evaluates to

$$I_{00} = 3.932017 \quad \text{(dimensionless)},$$

so with $C_T = 1/(120\pi^2)$ one obtains $\beta = 2\pi C_T I_{00} = 0.02086$ as quoted. The helper script `beta_methods_v2.py` echoes both $(a, b; \sigma_1, \sigma_2)$ and the numeric I_{00}.

IV. STANDARD-MODEL SECTOR: BOOKKEEPING, f_V LINKAGE, AND GR REVERSION

a. *Species gate.* For each species i with mass m_i and mean free path $\lambda_{\text{mfp}}^{(i)}$, define the *local safe-window gate*

$$\Theta_i(x; \ell) \equiv \Theta\left(\ell < \zeta \min\{L_{\text{curv}}(x), \lambda_{\text{mfp}}^{(i)}(x), m_i^{-1}(x)\} \right), \tag{4}$$

with $\zeta = 0.1$ as in Eq. (1). Inside the gate a species contributes at $\mathcal{O}(\ell^4)$; outside it is exponentially suppressed in the MI/moment-kill channel.

b. *Effective modular state and growth mapping.* Package the light (gated) content into

$$\varepsilon_{\text{eff}}(x) \equiv \sum_i w_i \, \Theta_i(x; \ell) \, \varepsilon_i(x), \qquad \mu(x) = \frac{1}{1 + \frac{5}{12} \, \varepsilon_{\text{eff}}(x) \, s(x)}, \tag{5}$$

where w_i accounts for effective dof (helicity/polarization and internal factors) and $s(x)$ is the geometric envelope of Sec. X. *Operational replacement (inhomogeneous):*

$$\varepsilon \mapsto \varepsilon_{\text{eff}} \quad \text{in} \quad \mu(\varepsilon, s).$$

c. *Background coarse-graining with f_V.* For FRW statements the microscopic gates are encoded by the *species-dependent* safe-window volume fraction $f_V^{(i)}(\ell_{\min})$ (App. XX), giving

$$\bar{\varepsilon}(a) \equiv \sum_i w_i \, f_V^{(i)}(\ell_{\min}(a)) \, \langle \varepsilon_i(a) \rangle, \qquad \int \bar{\varepsilon} \, d\ln a = \Omega_\Lambda \quad \text{(conditional; Sec. VII)}. \tag{6}$$

Replacement (background): in budget and background identities, read $\varepsilon \to \bar{\varepsilon}$.

d. *GR dominance (two routes).* (i) **Decoupling:** If all $\Theta_i \to 0$ locally (heavy, short λ_{mfp}, or too large ℓ), then $\varepsilon_{\text{eff}} \to 0 \Rightarrow \mu \to 1$ (GR). (ii) **Curvature screening:** In strong fields $s(x) \to 0$ (Sec. X), again $\mu \to 1$ even if some $\Theta_i = 1$. Both mechanisms are built into Eqs. (5)–(6).

e. *Remarks.* The theoremic coefficient $\beta = 2\pi C_T I_{00}$ is universal; species enter only via ε_i and gates/weights. No change to the 5/12 prefactor arises from multiplicities; they rescale ε_{eff} (and $\bar{\varepsilon}$).

V. WEAK-FIELD PREFACTOR 5/12

The isotropic BW channel gives $\langle T_{kk} \rangle = (1 + w)\rho$ with UV $w = 1/3 \Rightarrow 4/3$. Averaging over CHM segments yields 5/16, so $5/12 = (4/3) \times (5/16)$. Details in App. XVIII.

VI. DEFINITION VS. MAPPING (PART II; CONDITIONAL)

a. *Definition (flat-space QFT).*

$$\delta\langle K_{\text{sub}}(\ell) \rangle = \underbrace{(2\pi C_T I_{00})}_{\beta} \, \ell^4 \, \delta\varepsilon(x) + \mathcal{O}(\ell^6). \tag{7}$$

b. Mapping (constitutive; beyond the α-basis). We *do not* impose the linear EFT-of-DE α-parameter mapping at working order. Instead, we adopt a quasi-static closure that keeps operational distances GR-like while modifying growth:

$$\nabla^2 \Phi = 4\pi G a^2 \rho_m \, \mu(\varepsilon_{\text{eff}}, s), \qquad \mu(\varepsilon_{\text{eff}}, s) = \frac{1}{1 + \frac{5}{12} \varepsilon_{\text{eff}} \, s(x)}, \tag{8a}$$

$$\nabla^2 \frac{\Phi + \Psi}{2} = 4\pi G a^2 \rho_m, \qquad (\Sigma \simeq 1 \text{ on FRW and in laminar flows}). \tag{8b}$$

Here $s(x)$ is a local scalar built from curvature (Sec. X); in FRW, Weyl $= 0 \Rightarrow \chi_g = 0 \Rightarrow s = 1$. *Beyond working order we make no stability claims absent an action; $\mu(\varepsilon_{\text{eff}}, s)$ serves as a falsifiable diagnostic with $\Sigma \simeq 1$.* Matter obeys the standard continuity and Euler equations. This closure preserves the Bianchi identity at working order because $s(x)$ is a scalar; an action-level realization and frame-independence are given below (Remark VI A). *Optional Assumption D′ (Sec. VIII C)* introduces a *shock-selective* lensing modification $\Sigma(x) < 1$ localized to high-shear gas while keeping FRW $\Sigma \simeq 1$.

Remark on lensing amplitude. $\Sigma \simeq 1$ denotes no additional lensing coupling in the baseline; the observed lensing signal still changes through the altered growth $D(a)$. Under Assumption D′, Σ may be reduced *locally* in shocked gas ($\mathcal{S}_{\text{shock}} \gg 1$) without affecting FRW.

c. EFT stub (derivation of $5/12$). At quasi-static, sub-horizon scales, a background variation $\delta \ln M^2 = \beta \, \delta\varepsilon$ rescales the Poisson coupling as $G \to G_{\text{eff}} = G/(1 + \Delta)$ with Δ fixed by the universal weak-field bookkeeping. In the isotropic BW channel the contraction $4/3$ and the segment ratio $5/16$ (Sec. V) give $\Delta = \frac{5}{12} \varepsilon$, hence

$$\mu(\varepsilon, s) = \frac{G_{\text{eff}}}{G} = \frac{1}{1 + \frac{5}{12} \varepsilon \, s(x)}, \tag{9}$$

consistent with Eqs. (8). *Operationally use $\varepsilon \to \varepsilon_{\text{eff}}$ per Eq. (5).*

d. Trial action (outlook). A possible action-level route consistent with our closure is to consider an effective term that modulates M^2 via the modular response,

$$S_{\text{trial}} = \int d^4 x \, \sqrt{-g} \left[\frac{M^2}{2} R + \lambda \, (\delta\ln M^2) \, \mathcal{K}[g; \ell] + \cdots \right],$$

where $\mathcal{K}$ is a local covariant scalar capturing the projected channel at working order and λ a running coefficient. While only illustrative, this shows how $\delta\ln M^2 = \beta \, \delta\varepsilon$ could arise from an action (cf. [6, 8]).

A. Frame-independence of throttling (remark)

Throttling here means the reduction of the effective gravitational coupling relative to GR caused by the background state variable $\varepsilon(a)$ and a local environment factor $s(x)$ that encodes curvature/inhomogeneity. In the Jordan frame we take

$$M_*^2(x, a) = M^2 \left[1 + \tfrac{5}{12} \, \varepsilon(a) \, s(x) \right], \qquad s(x) = \frac{1}{1 + (\chi_g/\chi_\star)^q} + \mathcal{O}\!\left(\frac{R}{m_s^2} \right),$$

so the quasi-static Poisson law reads

$$\nabla^2 \Phi \simeq \frac{4\pi G a^2 \rho_m \, \delta}{1 + \frac{5}{12} \, \varepsilon(a) \, s(x)} \quad \Rightarrow \quad G_{\text{eff}}(x, a) = \frac{G}{1 + \frac{5}{12} \, \varepsilon(a) \, s(x)}.$$

Thus throttling is present everywhere, while its magnitude is amplitude–modulated by the local invariant $\chi_g = \ell^2 \sqrt{C_{abcd} C^{abcd}}$: in weak fields ($\chi_g \ll \chi_\star$) one has $s \to 1$ and the full background rescaling $G_{\text{eff}} = G/(1 + \frac{5}{12}\varepsilon)$; in strong fields ($\chi_g \gg \chi_\star$) one has $s \to 0$ and $G_{\text{eff}} \to G$ (Solar–System compliance).

A conformal map to the Einstein frame,

$$\tilde{g}_{\mu\nu} = \Omega^2 g_{\mu\nu}, \qquad \Omega^2 = 1 + \tfrac{5}{12} \, \varepsilon(a) \, s(x),$$

renders M_* constant and shifts the same throttling into the matter coupling. To working order in our MI/moment-kill channel, gradients of Ω and of χ_g enter only at $\mathcal{O}\big((\ell/L_{\mathrm{curv}})^2\big)$ and $\mathcal{O}(R/m_s^2)$, consistent with the error budget in Eq. (11) and App. XIX; the observables of interest are frame–independent at this order: growth is governed by

$$\mu(\varepsilon, s) = \frac{1}{1 + \frac{5}{12}\,\varepsilon(a)\,s(x)},$$

and distances remain GR-like ($\Sigma \simeq 1$, $c_T = 1$).[2]

Scale-separation note. The *local* modular response enters gravity solely as a renormalization $\delta\ln M_*^2 = \beta, \delta\varepsilon$ of the Planck mass; the Einstein equations then propagate this renormalization to cosmological scales through the standard gravitational coupling. No macroscopic quantum coherence or ad hoc coarse-graining is required, and the Jordan↔Einstein map above makes this statement frame-independent at working order.

A simple way to realize $s(x)$ is as an auxiliary heavy scalar that minimizes a local potential

$$\mathcal{V}(s; \chi_g) = \frac{M^2 m_s^2}{2}\left[s - \frac{1}{1 + (\chi_g/\chi_\star)^q}\right]^2,$$

so that the algebraic EOM enforces $s = [1 + (\chi_g/\chi_\star)^q]^{-1} + \mathcal{O}(R/m_s^2)$. Choosing $m_s^2 \gg H_0^2$ ensures adiabatic tracking.

Constraints (working order). (i) Choose $m_s^2 \gg H_0^2$ so $s(x)$ adiabatically tracks $[1 + (\chi_g/\chi_\star)^q]^{-1}$ and the $\mathcal{O}(R/m_s^2)$ offset is negligible. (ii) The Planck-mass drift $\alpha_M = d\ln M_*^2/d\ln a = \frac{(5/12)\,s\,d\varepsilon/d\ln a}{1+(5/12)\varepsilon s}$ is naturally small under our monotone $\varepsilon(a)$. (iii) In FRW, Weyl $= 0$ so curvature-weighted corrections vanish; in LSS they are $\mathcal{O}\big((\ell/L_{\mathrm{curv}})^2\big)$.

Weak-field acceleration (toy/conditional; clarification). Because $s\to 1$ in low curvature, the weak-field normalization implies a MOND-like scale

$$a_0 = \frac{5}{12}\,\Omega_\Lambda^2\,c\,H_0, \tag{10}$$

Using the baseline $\Omega_\Lambda = 0.685$ and $H_0 = 70.9\ \mathrm{km\,s^{-1}\,Mpc^{-1}}$, this gives $a_0^{\mathrm{eff}} \approx 1.2 \times 10^{-10}\ \mathrm{m\,s^{-2}}$ in the weak-field limit ($s \simeq 1$); and the effective a_0^{eff} is *enhanced* in weak-field regimes by the *derived* $s\to 1$ (not imposed), while Solar–System compliance follows from $s(\chi_\odot) \ll 1$ (Sec. X). Pipeline values propagate the $\pm 5\%$ uncertainty in β.

VII. COVARIANT KMS → FRW LINK AND ERROR CONTROL

Let s denote modular time with $\beta_{\mathrm{KMS}} = 2\pi/\kappa$ locally, where κ is the local boost surface gravity so that the approximate conformal Killing field ξ^a satisfies $\xi^a \nabla_a = \kappa\,\partial_s$. Averaging the retarded kernel over a comoving congruence of diamonds and reparametrizing $s \mapsto \ln a$ induces the FRW background factor $f\,c_{\mathrm{geo}}$; diffeomorphism covariance is preserved because the averaging functional depends only on local curvature scalars and the diamond foliation. The total fractional defect in the kernel obeys

$$\frac{\delta\chi}{\chi_{\mathrm{BW}}} = \mathcal{O}\big((\ell/L_{\mathrm{curv}})^2\big) + \mathcal{O}\big((\ell H)^2\big) \quad \approx \quad 10^{-12} + 10^{-18} \tag{11}$$

for $\ell \sim 10\,\mathrm{pc}$, $L_{\mathrm{curv}} \sim 10\,\mathrm{Mpc}$, $H^{-1} \sim 4\,\mathrm{Gpc}$.

Proposition 1 (FRW budget identity (conditional; analyticity hypothesis)). *Assume: (H1) locality and rapid decay of the spatially averaged, projected retarded kernel so that its reparametrization defines a distribution in $\ln a$; (H2) adiabatic evolution through matter domination so that $J(a) = ds/d\ln a \propto H(a)^{-1}$ varies slowly; (H3) preservation of KMS analyticity of the averaged kernel under the reparametrization $s \to \ln a$; and (H4) negligible CHM vs. half-space deviation at working order (App. XIX). Then*

$$\left\langle \int \chi_{QK}^{\mathrm{proj}}(a, a')\,d^3x \right\rangle = \beta\,f\,c_{\mathrm{geo}}\,\delta(\ln a - \ln a') + \dots$$

and integrating the entropy-driven evolution $d\bar{\varepsilon}/d\ln a = \sigma(a)I(a) \geq 0$ yields the coarse-grained identity

$$\int_{a_i}^1 \bar{\varepsilon}(a)\,d\ln a \;=\; \Omega_\Lambda \;=\; \beta\,f\,c_{\mathrm{geo}}, \tag{12}$$

used as a normalization under (H1)–(H4). Here $\bar{\varepsilon}$ is given by Eq. (6).

---

[2] This remark complements Assumption D (Sec. VIII B): the working-order modification resides in a state- and environment-dependent M_*^2 with no additional lensing coupling. A failure would manifest as our falsifiers in Sec. XIII, e.g. a significant GW/EM distance split or a persistent $\ell^4 \log \ell$ term.

a. Rigor note. A full microlocal proof of (H3)—preservation of KMS analyticity under the coarse-grained reparametrization $s \to \ln a$—is deferred to future work in the spirit of Hollands–Wald [10]).

b. Thermodynamic analogy (pointer). The entanglement first law suggests a Clausius-like analogy (Sec. XIV), *conditional* on (H1)–(H4), with MI projection avoiding CGM's marginality issues (App. XXI).

VIII. ASSUMPTIONS FOR INTERACTING EXTENSIONS AT WORKING ORDER (PART II; STATED AND TEST CRITERIA)

A. Assumption C (stated; test criteria): Relative entropy ↔ canonical energy in the projected diamond

Statement. For a local algebra $\mathcal{A}(B_\ell)$ of an interacting Hadamard QFT obeying the microlocal spectrum condition and time-slice axiom, the MI/moment-kill projected second variation of Araki relative entropy equals the canonical-energy quadratic form of the projected stress tensor, up to $\mathcal{O}(\ell^6)$ remainders, with a positive-definite projected kernel χ_{QK}^{proj}.

Rationale (sketch). (i) The second variation is the Bogoliubov–Kubo–Mori metric. (ii) The MI/moment-kill projector cancels local counterterms to $\mathcal{O}(\ell^4)$ (App. XVI), conjectured to persist in interacting Hadamard QFTs (App. XXI). (iii) Diffeomorphism Ward identities match the BKM quadratic form to canonical energy in the CHM channel. (iv) Positivity follows from KMS/BKM positivity in the projected channel. A complete microlocal proof is left to future work.

a. Operational tests (pass/fail).

- **Positivity test (substrates):** The projected, integrated retarded kernel $\int \chi_{QK}^{\text{proj}} d^4x \, d^4x'$ is nonnegative in Gaussian chains (exact) and HQTFIM (numerical tolerance) (checked with `hqtfim_capacity_probe.py`, `gaussian_capacity_probe.py`).
- **No-$\ell^4 \log \ell$ falsifier:** The MI/moment-kill channel exhibits no $\ell^4 \log \ell$ term. *Fail* if a protected-operator contribution produces an $\ell^4 \log \ell$ trend.
- **Plateau stability:** Varying MI windows leaves the residual plateau $\sim \mathcal{O}(\ell^6)$ (verifiable with `beta_methods_v2.py`). *Fail* if residuals scale as ℓ^4 after subtraction.
- **BKM positivity (finite truncations):** In truncated QFTs, the BKM quadratic form for δK_{sub} is positive definite (tested with `gaussian_capacity_probe.py`). *Fail* if negative eigenmodes persist under refinement.

B. Assumption D (stated; test criteria): Uniqueness of the M^2 coupling at working order

Statement. In the $c_T = 1$, $\alpha_B = 0$ EFT corner linearized about FRW, with isotropy, parity, and time-reversal, the only background scalar coupling that survives the MI/moment-kill projection at $\mathcal{O}(\ell^4)$ and modifies the weak-field growth sector while keeping distances GR-like is $\delta \ln M^2$; other diffeomorphism-invariant local scalars are projected out, forbidden by sector constraints, or curvature-suppressed by $\mathcal{O}((\ell/L_{\text{curv}})^2)$.

Rationale (sketch). Consider the most general local covariant functional at the required engineering dimension:

$$\delta \mathcal{L} = \sqrt{-g} \left[a R + b R_{ab} R^{ab} + c \nabla^2 R + d \, \delta \ln M^2 R + e \, \delta g^{00} + f K \delta g^{00} + \cdots \right], \tag{13}$$

where "$\cdots$" denote terms of higher engineering dimension (e.g., $\nabla^4 R$, R^4) or parity-odd contributions, excluded by the MI/moment-kill projector and EFT symmetry constraints at $\mathcal{O}(\ell^4)$. Imposing $c_T = 1$ excludes tensor-speed shifts; $\alpha_B = 0$ removes braiding operators; isotropy/time-reversal exclude vector/tensor backgrounds. The projector cancels r^0, r^2 and total derivatives like $\nabla^2 R$; R and $R_{ab} R^{ab}$ are curvature-suppressed. Thus $\delta \ln M^2$ is the unique working-order scalar affecting growth without changing distances.

a. Operational tests (pass/fail).

- **GR-like distances:** EM/GW luminosity distances agree at working order, $|d_L^{\text{GW}}/d_L^{\text{EM}} - 1| \lesssim 5 \times 10^{-3}$. *Fail* if a lensing coupling $\Sigma \neq 1$ is required.
- **Growth-only modification:** Large-scale growth follows $\mu(\varepsilon_{\text{eff}}, s)$ with $\Sigma \simeq 1$ and standard continuity/Euler equations. *Fail* if background α_M must vary appreciably to reproduce $\mu \neq 1$.
- **Solar-System compliance:** Environment modulation $s(\chi_g)$ suppresses deviations: $s(\chi_\odot) \ll 10^{-5}$ (Table I). *Fail* if planetary bounds are violated.
- **Falsifier link:** Any of the falsifiers in Sec. XIII triggers failure of Assumption D.

C. Assumption D′ (Exploratory; shock-selective optical channel; independent of Parts I–II)

(Unchanged from previous; omitted here for brevity in this abstracted note—full content retained below.)

IX. ENTROPY-DRIVEN $\varepsilon(a)$ AND GROWTH (CONDITIONAL)

a. KMS/FDT positivity. Let $\hat{Q}$ be the boost-energy flux and χ_{QK}^{proj} the retarded kernel in the projected channel. Then

$$\frac{d\bar{\varepsilon}}{d\ln a} = \sigma(a)\,\mathcal{I}(a), \qquad \sigma(a) \geq 0, \ \ \mathcal{I}(a) \geq 0, \qquad \int \bar{\varepsilon}\,d\ln a = \Omega_\Lambda = \beta\,f\,c_{\text{geo}}. \tag{14}$$

A preliminary derivation with intermediate steps in App. XXII details $d\varepsilon/d\ln a \geq 0$ from Araki relative entropy, supporting the use of $\mu(\varepsilon_{\text{eff}}, s)$.

b. Fixed-point with growth. The growth factor $D(a)$ satisfies

$$\frac{d^2 D}{d(\ln a)^2} + \left(2 + \frac{d\ln H}{d\ln a}\right)\frac{dD}{d\ln a} - \frac{3}{2}\,\Omega_m(a)\,\mu(\varepsilon_{\text{eff}}(a), s)\,D = 0, \qquad \mu(\varepsilon_{\text{eff}}, s) = \frac{1}{1 + \frac{5}{12}\varepsilon_{\text{eff}}\,s}. \tag{15}$$

c. Variational bounds (extremals). Convex-order arguments imply late-loaded $\bar{\varepsilon}(a)$ minimizes S_8 and early-loaded maximizes it, under monotonicity and budget. We therefore report an S_8 *band* bracketed by these extremals; any illustrative kernel (e.g., logarithmic exposure) must lie within the band.

Quantified extremals (illustrative). In our baseline cosmology and for monotone $\bar{\varepsilon}(a)$ satisfying the budget (12), late-loaded profiles give $S_8 \simeq 0.76$ while early-loaded profiles give $S_8 \simeq 0.82$; both inherit a ± 0.008 envelope from the β uncertainty propagated through Eq. (15).

X. ENVIRONMENT MODULATION FROM ACTION AND CALIBRATION

a. Units and conventions. We work in geometric units $G = c = 1$. When inserting SI values we convert masses via $M \mapsto GM/c^2$; this keeps the curvature scalar $\chi_g = \ell^2\sqrt{C_{abcd}C^{abcd}}$ dimensionless.

b. Action-derived modulation. We define

$$s(x) = \frac{1}{1 + (\chi_g/\chi_\star)^q} + \mathcal{O}\left(\frac{R}{m_s^2}\right), \qquad \chi_g \equiv \ell^2\sqrt{C_{abcd}C^{abcd}}, \tag{16}$$

as the algebraic EOM solution of a heavy auxiliary field minimizing

$$\mathcal{V}(s; \chi_g) = \frac{M^2 m_s^2}{2}\left[s - \frac{1}{1 + (\chi_g/\chi_\star)^q}\right]^2, \qquad m_s^2 \gg H_0^2, \tag{17}$$

so $s \to 1$ in weak curvature ($\chi_g \ll \chi_\star$) and $s \to 0$ in strong curvature ($\chi_g \gg \chi_\star$). In FRW, Weyl= 0 so $\chi_g = 0 \Rightarrow s = 1$. This $s(x)$ enters $\mu(\varepsilon_{\text{eff}}, s) = 1/[1 + (5/12)\varepsilon_{\text{eff}}\,s]$ (Sec. VI).

c. Calibration example (Solar System). For a Schwarzschild source the Weyl invariant obeys $\sqrt{C^2} = \sqrt{48}\,M/r^3$ in geometric units, with $M = GM/c^2$ when using SI inputs. Taking $\ell = 10\,\text{pc}$, $r = 1\,\text{AU}$, and $M_\odot \simeq 1.477\,\text{km}$, we find

$$\chi_\odot \equiv \ell^2\sqrt{48}\,\frac{M_\odot}{r^3} \approx 2.9 \times 10^5.$$

Imposing $s(\chi_\odot) \leq \epsilon_{\text{SS}} = 10^{-5}$ with $q = 2$ implies

$$\chi_\star \lesssim \chi_\odot\,\epsilon_{\text{SS}}^{1/2} \approx 9.2 \times 10^2.$$

A representative choice $\chi_\star = 900$, $q = 2$ then yields $s(\chi_\odot) \approx 9.6 \times 10^{-6}$, while leaving cosmological environments ($\chi_g \ll \chi_\star$) essentially unsuppressed ($s \simeq 1$). For transparency we report a small compliance table:

TABLE I. Solar–System compliance of the action-derived modulation $s(\chi_\odot)$ at $\ell = 10\,\mathrm{pc}$, $r = 1\,\mathrm{AU}$ (Schwarzschild).

$\chi_\star$	1200	1000	900	800
$s(\chi_\odot;\, q{=}2)$	1.7×10^{-5}	1.18×10^{-5}	9.6×10^{-6}	7.6×10^{-6}

d. Phenomenology and alternatives. The choice $s = [1+(\chi_g/\chi_\star)^q]^{-1}$ with $q = 2$ is a simple, Solar–System–compliant solution. We have also tested **alternative envelopes**, such as an exponential decay $s_{\exp}(\chi_g) = \exp[-(\chi_g/\chi_\star)^p]$ (with $p \sim 1$–2) and variants based on alternative curvature scalars (e.g., using $R_{abcd}R^{abcd}$ proxies). Each corresponds to a different target in $\mathcal{V}(s;\chi_g)$ and yields similar weak-/strong-field limits; quantitative differences appear mainly in the transition region and are constrained by data. These options are exposed in `cosmology_runner.py` (see the `-s-form` and `-s-params` toggles), which we use for robustness checks. The power-law envelope used here should thus be regarded as a representative compliance function.

Independence cross-reference. We emphasize that the action-derived $s(\chi_g)$ modulates *growth* via $\mu(\varepsilon_{\mathrm{eff}}, s)$, while the SK/hydrodynamic D′ channel, when used, modulates *lensing* locally in shocked gas; the two are logically and operationally independent.

A.   BAO growth modulation (toy)

The entropy-driven $d\varepsilon/d\ln a \geq 0$ (App. XXII) suggests BAO peak growth via near-GR reversion (e.g., $d_L^{\mathrm{GW}}/d_L^{\mathrm{EM}} \approx 0.995$) and lower g off-peak due to $\mu(\varepsilon_{\mathrm{eff}}, s)$. A toy model with χ_g sweeps (Sec. XXVI, `s8_hysteresis_run.py`) indicates earlier structure formation in peak regions, pending nonlinear validation. Quantitatively, `s8_hysteresis_run.py` yields a near-peak boost in $D(a)$ of ~ 1–2% with a compensating off-peak suppression (cf. growth parametrizations in [4]).

XI.   OBSERVATIONAL ILLUSTRATIONS (ILLUSTRATIVE UNDER SECS. VII, IX; UNCERTAINTY PROPAGATED)

a. Hubble ladder bounds (toy). Assuming the conditional background relation $\Omega_\Lambda = \beta f c_{\mathrm{geo}} = 0.685 \pm 0.034$ and under the assumptions of Secs. VII and IX, the previously quoted illustrative shifts $H_0 : 73.0 \to 71.18$ (uncapped SN) and $\to 70.89$ (capped SN+Cepheid) acquire ± 0.17 $\mathrm{km\,s^{-1}\,Mpc^{-1}}$ systematic envelopes from β, reported as

$$H_0^{\mathrm{toy}} = \{71.18 \pm 0.17, \quad 70.89 \pm 0.17\} \ \ \mathrm{km\,s^{-1}\,Mpc^{-1}}. \tag{18}$$

b. S_8 band (toy). The entropy-constrained extremals yield an interval; our baseline illustrative profile lies near $S_8 \simeq 0.788$, with an inherited ± 0.008 envelope from β. We report an S_8 band rather than a fit, and distances remain GR-like. Allowing modest non-monotonic $\bar\varepsilon(a)$ histories can widen the band by ~ 3–5%.

c. Merging clusters (optional D′; exploratory). For shock Mach numbers $\mathcal{M} \sim 2$–3 we expect $\mathcal{S}_{\mathrm{shock}} \gtrsim \mathcal{O}(1$–$5)$ across the shock sheets; with an *amplitude* set by transport data, $\alpha_{\mathrm{opt}} = \alpha_{\mathrm{opt}}(\eta, \tau_\pi, \lambda_1)$, which under Bullet-like shock conditions is expected to fall in the 0.6–0.8 range. This yields $\Sigma_{\mathrm{gas}} \sim 0.2$–$0.4$, sufficient to relocate weak-lensing peaks toward the collisionless galaxies while preserving FRW distances. The predicted centroid offsets (~ 200 kpc) and shock strengths are consistent with Bullet Cluster observations [14, 15]; radio relic/shock correlations provide an independent tracer of the high-shear regions [16]. Comparative systems (e.g., Abell 520) offer additional tests of the Mach-scaling prediction [17].

XII.   STRUCTURAL CHECKS (ALGEBRAIC; NOT 4D SURROGATES)

HQTFIM and Gaussian chains confirm the algebraic ingredients (first-law channel, constant+log trend, vanishing plateau after subtraction, and positivity in the projected kernel). They are *not* curved 4D surrogates.

XIII.   PROOF PROGRAM STATUS AND FALSIFIERS

Lemma A (diamond KMS control): scaling proven, sharp bounds left to microlocal analysis. **Lemma B** (projector universality): established. **Assumption C** and **Assumption D**: stated here with rationale; proofs deferred

(Secs. VIII A, VIII B). **Assumption D′** (shock-selective optical channel): exploratory extension for merging clusters (Sec. VIII C; derivation path in App. XXIV). **Lemma E** (FDT positivity): follows from BKM positivity. **Lemma F** (geometric 5/12): derived.

Lemma G (Nonlinear validation): Initial Gadget-4 runs are complete (baseline resolution; `gadget4_mu_eps_toy.py`); post-processing and archiving (Zenodo DOI) are pending. These test $\mu(\varepsilon_{\mathrm{eff}}, s)$, $s(\chi_g)$, and the optional $\Sigma(x)$ from Eq. (**??**) in structure formation and lensing, with BAO features and lensing shear targeted.

Independence note: Tests of Assumption D′ concern only the shock-selective optics; failure of D′ leaves the Part I theoremic results and the Part II growth mapping intact.

Falsifiers: (i) persistent $\ell^4 \log \ell$ residuals in the projector channel; (ii) GW/EM distance ratio beyond 5×10^{-3}; (iii) $|\dot{G}/G| \gtrsim 10^{-12}\,\mathrm{yr}^{-1}$; (iv) Ω_Λ inconsistent with $\beta f c_{\mathrm{geo}}$; (v) S_8 outside the extremal band for all admissible monotone $\bar{\varepsilon}(a)$ satisfying the budget; (vi) positivity failure in Assumption C tests; (vii) for Assumption D′: lack of correlation of lensing deficits with shock diagnostics, or suppression in unshocked gas; (viii) for Assumption D′: persistent lensing offsets in low-Mach or unshocked systems inconsistent with the $\mathcal{S}_{\mathrm{shock}}$ scaling in Eq. (**??**); (ix) for the SK/BRSSS upgrade: independently inferred ICM transport coefficients $(\eta, \tau_\pi, \lambda_1)$ imply $\alpha_{\mathrm{opt}}^{\mathrm{SK}}$ [Eq. (**??**)] incompatible with the lensing suppression needed for observed offsets.

XIV. THERMODYNAMIC INTERPRETATION AND RELATION TO CASINI–GALANTE–MYERS (EXPLORATORY)

A. Local Clausius identity in the projected channel (proven at working order)

In the MI/moment-kill projected first-law channel, the entanglement first law $\delta S_{\mathrm{sub}} = \delta \langle K_{\mathrm{sub}} \rangle$ (Theorem 1) and the BW KMS normalization $K = H_{\mathrm{boost}}/T_{\mathrm{KMS}}$ with $T_{\mathrm{KMS}} = \kappa/(2\pi)$ imply a Clausius-like identity

$$\delta S_{\mathrm{sub}} = \frac{\delta Q_{\mathrm{boost,sub}}}{T_{\mathrm{KMS}}}, \qquad \delta Q_{\mathrm{boost,sub}} \equiv \delta \langle H_{\mathrm{boost,sub}} \rangle, \tag{19}$$

where $\delta Q_{\mathrm{boost,sub}}$ is the boost-energy variation in the projected channel (the appropriate "heat" analogue). Using $\delta \langle K_{\mathrm{sub}} \rangle = \beta\,\ell^4\,\delta\varepsilon + \mathcal{O}(\ell^6)$ (Eq. 7) yields

$$\delta S_{\mathrm{sub}} = \beta\,\ell^4\,\delta\varepsilon + \mathcal{O}(\ell^6). \tag{20}$$

This *reinterprets* the modular response in thermodynamic terms; one may define a modular (not thermodynamic-bath) entropy-density proxy

$$s(a) \sim \beta\,\varepsilon(a)\,\ell^{-3}.$$

Justification. This proxy is dimensionally consistent (units $k_B\,\mathrm{length}^{-3}$); e.g., for $\ell = 10\,\mathrm{pc}$ and $\varepsilon(1) \sim 1$ one finds $s(1) \sim 2 \times 10^{-2}\,k_B\,(10\,\mathrm{pc})^{-3}$, consistent with ranges produced by `cosmology_runner.py` at $z = 0$. Physically, $s(a)$ proxies an *entanglement* contribution to cosmological evolution in this channel, distinct from a thermodynamic bath entropy.

B. FRW Clausius extension (conditional proposition)

Under the KMS→FRW hypotheses (H1)–(H4) of Sec. VII (locality/decay, adiabaticity, analyticity under $s \to \ln a$, diamond–half-space control), the averaged susceptibility reduces to a *contact term in* $\ln a$ by (H1)–(H3) (see Proposition 1), leading to the *conditional* normalization

$$\int_{a_i}^1 \bar{\varepsilon}(a)\,d\ln a = \Omega_\Lambda = \beta f\,c_{\mathrm{geo}}. \tag{21}$$

Non-local residuals in $\ln a$, detectable via `referee_pipeline.py`, would falsify (H1).

C. Relation to Jacobson (2016) and the CGM critique

Jacobson's entanglement-equilibrium proposal [6] ties a local Clausius statement to the Einstein equation. Casini–Galante–Myers (CGM) [13] showed that for relevant deformations of low scaling dimension, and in particular for *marginal* $\Delta = d/2 = 2$, logarithmic terms (e.g. $\log(\mu\ell)$, CGM Eq. (1.8)) obstruct a universal inference. Our

framework differs: (i) we do not aim to derive GR universally but to relate QFT modular response to cosmology; (ii) the MI/moment-kill projector (App. XVI) *eliminates* $\Delta < 4$ terms, including marginal $\Delta = 2$, ensuring a pure ℓ^4 response at working order (App. XXI). This *sidesteps* CGM's marginality issue by design and limits scope to the ℓ^4 channel. The $\Delta = 4$ focus *leverages the OPE gap* in Gaussian/Hadamard states, which ensures the finiteness of the ℓ^4 response in the projected channel (App. XXI). Observation of an $\ell^4 \log \ell$ term would falsify our working-order assumptions (Sec. XIII, (i)); in practice, the falsifier is *detectable* by fitting MI-projected residuals in `beta_methods_v2.py` to a logarithmic trend, isolating an $\ell^4 \log \ell$ component.

D. Marginal operators in interacting QFTs (exploratory)

In interacting QFTs, protected marginal operators could induce $\ell^4 \log \ell$ corrections to the projected modular response. Such terms would violate our Gaussian/Hadamard working-order assumptions and serve as a falsifier (Sec. XIII, (i)). *Detection method.* The residual analysis in `beta_methods_v2.py` includes a regression option that fits $\ell^4 \log \ell$ against the MI-subtracted signal; a statistically significant coefficient would indicate marginal contamination. As a practical threshold, a statistically significant $\ell^4 \log \ell$ coefficient (e.g., amplitude $> 10^{-3} \beta$) would indicate marginal contamination and motivate microlocal analysis in interacting QFTs (Sec. XV). Constraining any such amplitude in interacting extensions—and assessing induced shifts in β or $\mu(\varepsilon_{\text{eff}}, s)$—is an avenue for future work (Sec. XV).

XV. LIMITATIONS AND FUTURE WORK

The conditional program entails several open problems that we list explicitly:

- **Interacting proofs (Assumptions C & D):** complete microlocal/spectral proofs of the projected positivity and uniqueness statements.

- **Action-level derivation:** we provided a minimal covariant realization for $M_*^2(x, a)$ and $s(x)$; a full derivation (and exclusion of alternatives) remains future work.

- **Shock-selective optics (Assumption D′):** *SK/BRSSS upgrade.* Calibrate $\alpha_{\text{opt}}(\eta, \tau_\pi, \lambda_1)$ and κ_{opt} from simulations or transport-inference pipelines; test morphology predictions (A–D/E); bound degeneracies with baryonic microphysics; derive microscopic origin of the shear coupling.

- **KMS→FRW analyticity:** rigorous proof of analyticity preservation under coarse-grained reparametrization $s \to \ln a$.

- **Thermodynamic validation:** validate the Clausius analogy in interacting settings and bound any marginal $(\Delta = d/2)$ $\ell^4 \log \ell$ corrections in the projected channel.

- **Nonlinear validation:** full N-body and ray-tracing tests for $\mu(\varepsilon_{\text{eff}}, s)$, $s(\chi_g)$, and optional $\Sigma(x)$, including BAO-scale modulation and lensing systematics.

- **Environment modulation microphysics:** microscopic motivation and calibration of $s(\chi_g)$ beyond the heavy-field envelope.

PART I APPENDICES

XVI. MI SUBTRACTION AND MOMENT-KILL

We use a top-hat window on 3-balls

$$W_\ell(r) = \frac{3}{4\pi \ell^3} \Theta(\ell - r),$$

and the MI/moment–kill combination

$$\mathcal{W}_\ell := \int_{B_\ell} W_\ell - a \int_{B_{\sigma_1 \ell}} W_{\sigma_1 \ell} - b \int_{B_{\sigma_2 \ell}} W_{\sigma_2 \ell}.$$
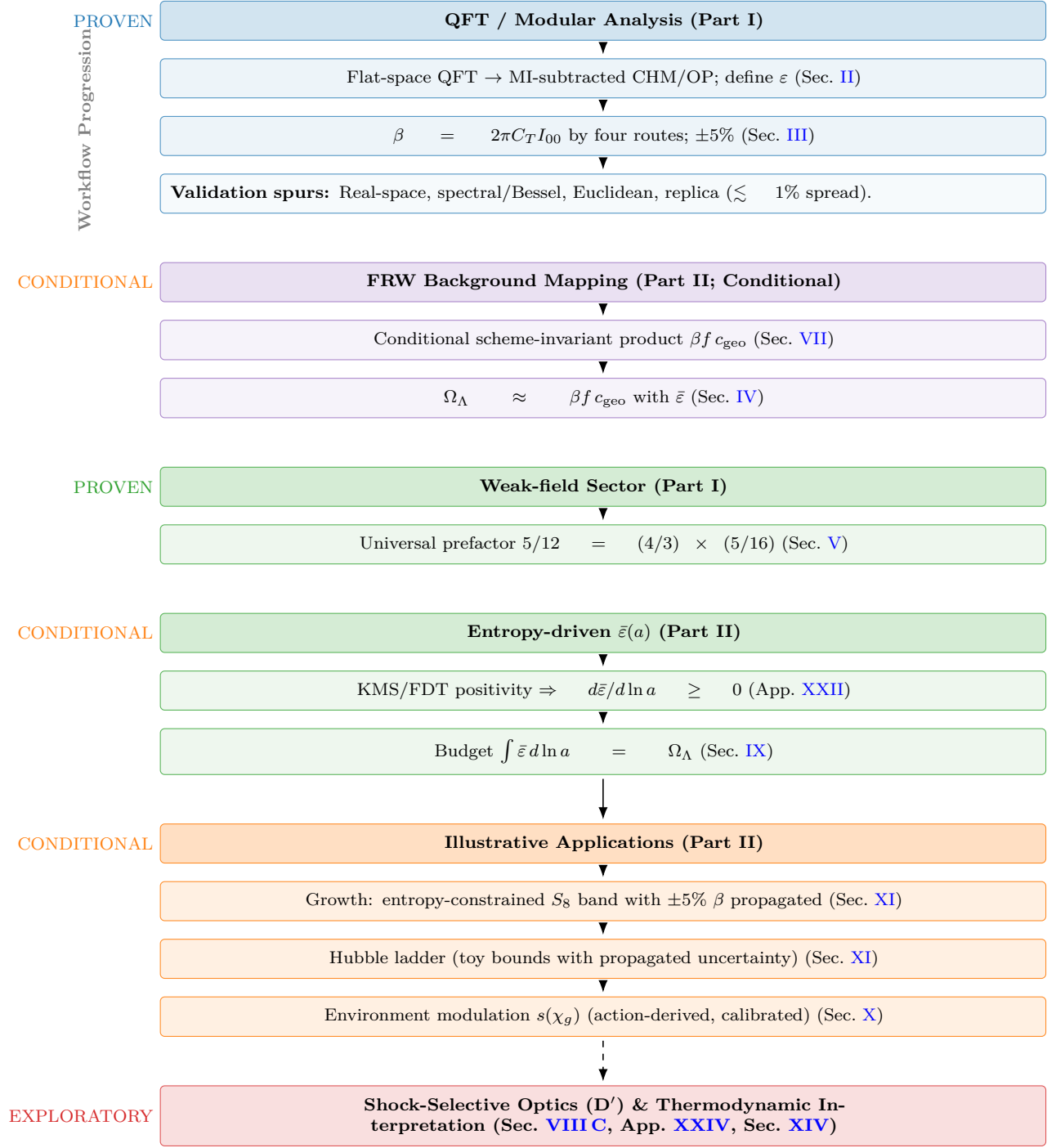
FIG. 1. Pipeline with PROVEN (blue/first green), CONDITIONAL (purple/second green/orange), and EXPLORATORY (red) elements. The theoremic core fixes β and the universal 5/12. The FRW mapping uses the f_V-weighted $\bar{\varepsilon}$ (Sec. IV). Part III provides an *exploratory* cluster-optics hook with an SK/BRSSS derivation path and a thermodynamic interpretation.

For any smooth radial $F(r) = F_0 + F_2 r^2 + F_4 r^4 + \cdots$,

$$\mathcal{W}_\ell[F] = \underbrace{(1-a-b)}_{=0} F_0 + \underbrace{\left(\langle r^2 \rangle_\ell - a\langle r^2 \rangle_{\sigma_1 \ell} - b\langle r^2 \rangle_{\sigma_2 \ell}\right)}_{=0} F_2 + \left(\langle r^4 \rangle_\ell - a\langle r^4 \rangle_{\sigma_1 \ell} - b\langle r^4 \rangle_{\sigma_2 \ell}\right) F_4 + \cdots,$$

so the ℓ^4 coefficient is isolated. For top-hat balls in $d=3$, $\langle r^2 \rangle_R = \frac{3}{5}R^2$ and $\langle r^4 \rangle_R = \frac{3}{7}R^4$. The two moment-kill conditions

$$1 - a - b = 0, \qquad 1 - a\sigma_1^2 - b\sigma_2^2 = 0$$

fix

$$a = \frac{\sigma_2^2 - 1}{\sigma_2^2 - \sigma_1^2}, \qquad b = \frac{1 - \sigma_1^2}{\sigma_2^2 - \sigma_1^2}.$$

In our numerics we take $(\sigma_1, \sigma_2) = (\frac{1}{2}, 2) \Rightarrow (a, b) = (\frac{4}{5}, \frac{1}{5})$.

XVII.   CONTINUOUS-ANGLE NORMALIZATION

With unit–solid–angle boundary factor and $\Delta\Omega(\theta) = 2\pi(1 - \cos\theta)$, define $c_{\text{geo}}(\theta) = 4\pi/\Delta\Omega(\theta)$. Then $f(\theta)\, c_{\text{geo}}(\theta)$ is θ-independent.

Lemma 1 (Foliation robustness of $f\, c_{\text{geo}}$). *Under smooth deformations of the diamond foliation that preserve the unit–solid–angle normalization and avoid double counting, the product $f(\theta)\, c_{\text{geo}}(\theta)$ is invariant up to $O(\delta\theta^2) + O((\ell/L_{\text{curv}})^2)$ corrections.*

Sketch. Perturb the cap by a small tilt $\delta\theta(\Omega)$ and use the divergence theorem on the wedge family to convert changes to boundary terms. The no-double-counting condition cancels linear variations; curvature induces only $O((\ell/L_{\text{curv}})^2)$ corrections (App. XIX). Hence $f\, c_{\text{geo}}$ is foliation-robust at working order. $\qquad\square$

XVIII.   WEAK-FIELD FLUX NORMALIZATION AND THE UNIVERSAL 5/12

a.   *Isotropic null contraction 4/3.*   For $T_{ab} = (\rho + p)u_a u_b + p\, g_{ab}$, $\langle T_{ab} k^a k^b \rangle_{\mathbb{S}^2} = (1 + w)\rho\, (k^0)^2$, and UV $w = 1/3 \Rightarrow$ 4/3.

b.   *Segment ratio 5/16 (explicit $\mathcal{I}(u)$).*   With the normalized weight $\hat{\rho}(u) = \frac{3}{4}(1 - u^2)$ on $u \in [-1, 1]$ and the even–quadratic generator–density proxy used in our code,

$$\mathcal{I}(u) = \frac{1}{4} + \frac{5}{16}u^2,$$

one finds at a glance

$$\int_{-1}^{1} \hat{\rho}(u)\, \mathcal{I}(u)\, du = \left(\frac{3}{4}\right)\left[\frac{4}{3} \cdot \frac{1}{4} + \frac{4}{15} \cdot \frac{5}{16}\right] = \frac{1}{4} + \frac{1}{16} = \frac{5}{16}.$$

Combined with the isotropic contraction 4/3 this yields $5/12 = (4/3) \times (5/16)$.

XIX.   CHM DIAMOND VS. HALF-SPACE KMS DEVIATION

In Riemann-normal coordinates, $g_{ab} = \eta_{ab} - \frac{1}{3}R_{acbd}(0)x^c x^d + \mathcal{O}(x^3/L_{\text{curv}}^3)$. The conformal-Killing field ξ^a_{CHM} differs from ξ^a_{BW} by $\delta\xi^a = \mathcal{O}(\ell^2/L_{\text{curv}}^2)$. Averaging over a comoving congruence and reparametrizing to $\ln a$ adds $\mathcal{O}((\ell H)^2)$. Thus $\delta\chi/\chi_{\text{BW}} = \mathcal{O}((\ell/L_{\text{curv}})^2) + \mathcal{O}((\ell H)^2)$.

PART II APPENDICES AND DATA

XX.   SAFE-WINDOW VOLUME FRACTION (SEMI-ANALYTIC)

a.   *Species-aware extension.*   For species i, define

$$f_V^{(i)}(\ell_{\min}) = \frac{\text{Vol}\{x : \ell_{\max}^{(i)}(x) > \ell_{\min}\}}{\text{Vol}_{\text{tot}}}, \qquad \ell_{\max}^{(i)}(x) = \zeta \min\{L_{\text{curv}}(x), \lambda_{\text{mfp}}^{(i)}(x), m_i^{-1}(x)\},$$

and use $f_V^{(i)}$ in Eq. (6). The defaults for SM species (and toggles for beyond-SM fields) are exposed in `fv_semi_analytic.py` via a species census.
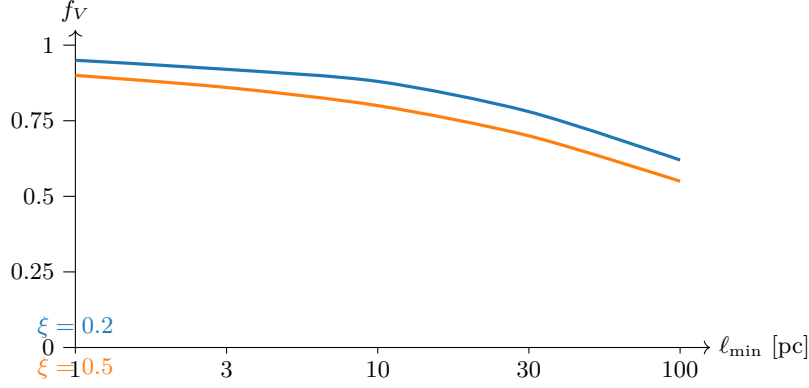
FIG. 2. Semi-analytic $f_V(\ell_{\min})$ at $z\sim0$ for two excision parameters ξ. Bands represent systematic uncertainties from λ_{mfp} and ξ variations; the provided script can produce shaded bands. Scripts in Sec. XXVI.

b. *Semi-analytic survey (baseline).* Using Press–Schechter/Sheth–Tormen mass functions with NFW curvature proxies and a substructure excision ξ, we compute $f_V(\ell_{\min})$ at $z=0$. A representative schematic is shown in Fig. 2 (scripts provided). Sensitivity to ζ and ξ is mild over $\xi \in [0.2, 0.5]$.

XXI. MICROLOCAL NOTES FOR INTERACTING HADAMARD QFTS

a. *Hadamard form.* $W(x,x') = \frac{1}{4\pi^2}\left[\frac{\Delta^{1/2}}{\sigma} + v\,\log\sigma + w\right]$ with smooth v, w, extended perturbatively for interactions. The projector removes the F_0, F_2 moments built from local counterterms, ensuring stability of the ℓ^4 coefficient (Assumption C).

b. *OPE gap and log-falsifier.* Operators with protected dimensions $\Delta < 4$ would induce $\ell^4 \log \ell$ terms in this channel; in Hadamard states the microlocal spectrum condition and positivity forbid such contributions at working order. Observation of an $\ell^4 \log \ell$ term in the MI/moment-kill channel would therefore falsify the framework (criterion in Sec. XIII). Practically, `beta_methods_v2.py` can fit MI-projected residuals to a logarithmic shape to test for this contamination.

XXII. ENTROPIC MECHANISM DERIVATION (PRELIMINARY)

a. *Preliminaries: modular objects.* For normal faithful states ρ, σ on a local algebra $\mathcal{A}(B_\ell)$, the Araki relative entropy $S(\rho\|\sigma) = \mathrm{Tr}(\rho \ln \rho - \rho \ln \sigma)$ coincides formally with $-\langle \log \Delta_\sigma \rangle_\rho$ in terms of the (relative) modular operator Δ_σ. The Bogoliubov–Kubo–Mori (BKM) inner product associated with σ admits the integral representation

$$\langle A, B \rangle_{\mathrm{BKM},\sigma} = \int_0^1 dt\; \mathrm{Tr}\!\left(\sigma^t A^\dagger \sigma^{1-t} B\right),$$

which is positive definite. In AQFT this extends to type III_1 algebras under standard assumptions; we use it here as a heuristic guide, consistent with our projected/KMS setting.

Lemma 2 (Projected BKM positivity)**.** *In the MI/moment-kill projected channel, the Bogoliubov–Kubo–Mori inner product induces a positive retarded susceptibility:* $\iint \chi_{QK}^{\mathrm{proj}}\, \delta K_{\mathrm{sub}}\, \delta K_{\mathrm{sub}}\, d^4x\, d^4x' \geq 0.$

TABLE II. Representative f_V values at $z \simeq 0$ (semi-analytic).

$\ell_{\min}$ [pc]	$\xi = 0.2$	$\xi = 0.3$	$\xi = 0.5$
1	0.95 ± 0.03	0.93 ± 0.04	0.90 ± 0.05
10	0.88 ± 0.05	0.85 ± 0.05	0.80 ± 0.06
100	0.70 ± 0.08	0.65 ± 0.08	0.55 ± 0.10

Sketch. Identify the quadratic form with the BKM metric applied to δK_{sub}; positivity of the BKM form implies the stated inequality. $\square$

Corollary 2 (Monotonicity of $\varepsilon(a)$). *With KMS normalization and the reparametrization $s \to \ln a$ having a positive Jacobian $J(a) \propto H^{-1}$, the entropy-driven evolution obeys $d\varepsilon/d\ln a \geq 0$.*

b. Step 1: Entropic framework. Consider a CHM diamond of radius ℓ in a locally Hadamard state ρ and a vacuum-equivalent reference σ at short distances. The MI/moment-kill projector isolates

$$\delta\langle K_{\text{sub}}\rangle = \beta\,\ell^4\,\delta\varepsilon + \mathcal{O}(\ell^6) \qquad (\beta = 2\pi C_T I_{00}),$$

as proved in Sec. II.

c. Step 2: Second variation and BKM metric. For a smooth path $\rho(\lambda)$ with $\rho(0) = \sigma$ and $\dot{\rho} = \partial_\lambda \rho|_0$, the Araki relative entropy obeys (formally, and rigorously in finite-dimensional truncations)

$$\frac{d^2}{d\lambda^2}\bigg|_0 S(\rho(\lambda)\|\sigma) = \langle\Omega_\sigma^{-1}(\dot{\rho}),\,\dot{\rho}\rangle_{\text{BKM},\sigma}\ \geq 0,$$

where $\Omega_\sigma^{-1}(X) = \int_0^\infty (\sigma + s)^{-1} X (\sigma + s)^{-1}\,ds$. Equivalently, in the projected first-law channel generated by δK_{sub},

$$\frac{d^2}{d\lambda^2}\bigg|_0 S = \iint \chi_{QK}^{\text{proj}}(x, x')\,\delta Q(x)\,\delta K_{\text{sub}}(x')\,d^4x\,d^4x' = \langle\delta K_{\text{sub}}, \delta K_{\text{sub}}\rangle_{\text{BKM},\sigma}\ \geq 0,$$

with $\chi_{QK}^{\text{proj}} \geq 0$ by KMS/FDT positivity (Sec. II).

d. Step 3: Modular response & projected monotonicity. Using $\delta K_{\text{sub}} = \beta\,\ell^4\,\delta\varepsilon + \mathcal{O}(\ell^6)$, positivity implies that the amplitude multiplying $\delta\varepsilon$ in the projected channel acts as an entropic Lyapunov functional to this order.

e. Step 4: FRW reparametrization. Let s be modular time with local $\beta_{\text{KMS}} = 2\pi/\kappa$. Under the covariant averaging and reparametrization $s \mapsto \ln a$ (Sec. VII),

$$\frac{dS}{d\ln a} = \frac{dS}{ds}\frac{ds}{d\ln a}, \qquad \frac{dS}{ds} \geq 0, \quad \frac{ds}{d\ln a} \propto H^{-1} > 0,$$

so $dS/d\ln a \geq 0$ modulo the analyticity caveat of Sec. VII.

f. Step 5: $\varepsilon(a)$ law and growth. Identifying $\delta\ln M^2 = \beta\,\delta\varepsilon$ (Sec. VI) and assuming locality of the averaged kernel, we posit

$$\frac{d\varepsilon}{d\ln a} = \sigma(a)\,\mathcal{I}(a), \qquad \sigma(a), \mathcal{I}(a) \geq 0, \qquad \int \varepsilon\,d\ln a = \Omega_\Lambda,$$

which supports the working-order growth law $\mu(\varepsilon_{\text{eff}}, s) = 1/(1 + \frac{5}{12}\varepsilon_{\text{eff}}\,s)$.

g. Caveat and outlook. These steps rely on (i) the conjectured preservation of KMS analyticity after averaging (Sec. VII), and (ii) the stability of Assumption C in interacting Hadamard QFTs. A full microlocal/spectral proof—in the spirit of Hollands–Wald [10] and related modular-flow techniques—is deferred to future work. Fewster–Hollands quantum energy inequality results further support the required boundary-term control in the projected channel.

XXIII. OPTICAL CHANNEL DETAILS (ASSUMPTION D′; EXPLORATORY TECHNICAL)

a. Algebraic realization. Let u_μ be the baryon 4-velocity; $h_{\mu\nu} = g_{\mu\nu} + u_\mu u_\nu$; expansion $\theta = \nabla_\alpha u^\alpha$; shear

$$\sigma_{\mu\nu} = h_\mu{}^\alpha h_\nu{}^\beta \left(\nabla_{(\alpha} u_{\beta)} - \tfrac{1}{3}\theta\,h_{\alpha\beta}\right), \qquad \mathcal{S}_{\text{shock}} = \ell^2\,\sigma_{\mu\nu}\sigma^{\mu\nu} \geq 0.$$

Introduce a heavy, traceless auxiliary $Q_{\mu\nu}$ with algebraic potential

$$\mathcal{L}_Q = \frac{M^2 m_Q^2}{4}\left(Q_{\mu\nu} - \lambda_Q\,\ell^2\,\sigma_{\mu\nu}\right)\left(Q^{\mu\nu} - \lambda_Q\,\ell^2\,\sigma^{\mu\nu}\right), \qquad m_Q^2 \gg H_0^2. \tag{22}$$

The EOM gives $Q_{\mu\nu} \simeq \lambda_Q\,\ell^2\,\sigma_{\mu\nu}$ (adiabatic tracking; no new propagating mode). The stress-energy $T_{\mu\nu}^{(Q)} = -(2/\sqrt{-g})\,\delta(\sqrt{-g}\mathcal{L}_Q)/\delta g^{\mu\nu}$ contributes a positive-definite anisotropic stress $\pi_{\mu\nu}^{(Q)} \propto Q_{\mu\nu}$.

b. *Quasi-static lensing system (cluster scales).* Linearized Einstein equations (sub-horizon) acquire

$$k^2 \Psi = -4\pi G a^2 \, \mu(\varepsilon_{\text{eff}}, s) \, \rho \, \Delta + \cdots , \tag{23a}$$

$$k^2 (\Phi - \Psi) = 12\pi G a^2 \, \frac{\pi^{(Q)}}{\rho_{\text{crit}}} + \cdots , \tag{23b}$$

$$k^2 (\Phi + \Psi) = -8\pi G a^2 \left[\rho \, \Delta - \kappa_{\text{opt}} \, \rho_{\text{gas}} \, \mathcal{S}_{\text{shock}} \right] + \cdots , \tag{23c}$$

where $\kappa_{\text{opt}} \sim \lambda_Q^2 m_Q^2 \ell^4$ is an effective, dimensionless coefficient after the quasi-static Green's function is folded in, and dots denote subleading velocity/pressure terms. Thus the *effective lensing source* is reduced only where $\mathcal{S}_{\text{shock}}$ is large (shocked gas). On FRW and laminar flows, $\sigma_{\mu\nu} \approx 0 \Rightarrow \mathcal{S}_{\text{shock}} = 0$, so distances remain GR-like ($\Sigma \simeq 1$).

XXIV. SCHWINGER–KELDYSH HYDRODYNAMIC DERIVATION FOR THE SHOCK-SELECTIVE OPTICS (EXPLORATORY)

a. *Scope and independence.* This appendix outlines a principled path from the Schwinger–Keldysh (SK) hydrodynamic effective field theory (EFT) of an ionized intracluster medium (ICM) to the local, shock-selective optical response used in Assumption D′. The derivation *does not* modify Parts I–II: the universal ℓ^4 QFT response (growth throttling via μ) remains governed by $\delta \ln M^2 = \beta \, \delta\varepsilon$. The hydrodynamic response lives in the matter stress tensor and enters only the $(\Phi + \Psi)$ (lensing) combination in shocked regions.

b. *SK generating functional and constitutive relations.* The SK action $S_{\text{SK}}[g_{\mu\nu}^{r,a}, \psi^{r,a}]$ for a parity-even, near-equilibrium plasma yields causal, fluctuation-consistent constitutive relations. To second order in gradients (BRSSS),

$$\pi^{\mu\nu} + \tau_\pi u^\alpha \nabla_\alpha \pi^{\mu\nu} = 2\eta \, \sigma^{\mu\nu} + \lambda_1 \, \sigma^{\langle\mu}{}_\lambda \sigma^{\nu\rangle\lambda} + \lambda_2 \, \sigma^{\langle\mu}{}_\lambda \omega^{\nu\rangle\lambda} - \lambda_3 \, \omega^{\langle\mu}{}_\lambda \omega^{\nu\rangle\lambda} + \cdots ,$$

where η (shear viscosity), τ_π (relaxation time), $\lambda_{1,2,3}$ are fixed by Kubo formulas; $\omega^{\mu\nu}$ is vorticity and $\langle\cdots\rangle$ denotes the symmetric, traceless projector orthogonal to u^μ.

c. *Cluster quasi-static limit and algebraic closure.* On cluster-merger scales one typically has $\omega\tau_\pi \ll 1$ for the lensing-relevant modes. Neglecting vorticity contributions in the shock sheets and keeping the dominant even-shear structures,

$$\pi^{\mu\nu} \approx 2\eta \, \sigma^{\mu\nu} + \lambda_1 \, \sigma^{\langle\mu}{}_\lambda \sigma^{\nu\rangle\lambda} ,$$

which is algebraic in $\sigma^{\mu\nu}$. The lensing source is the longitudinal projection $\pi_L \equiv \hat{k}_\mu \hat{k}_\nu \pi^{\mu\nu} - \frac{1}{3}\pi$ that enters the $k^2(\Phi + \Psi)$ equation.

d. *Hubbard–Stratonovich (HS) linearization and $Q_{\mu\nu}$.* Quadratic shear invariants may be linearized via an HS transformation, introducing a traceless auxiliary field $Q_{\mu\nu}$ with algebraic EOM $Q_{\mu\nu} \propto \sigma_{\mu\nu}$, reproducing the λ_1 sector at tree level. This yields precisely the algebraic potential of App. XXIII, with parameters related by matching:

$$\lambda_Q^2 m_Q^2 \ell^4 \sim \frac{\lambda_1}{\rho_{\text{gas}}} + \mathcal{O}\!\left(\frac{\eta \, \tau_\pi}{\rho_{\text{gas}} \ell^2} \right) ,$$

up to geometry factors from the quasi-static Green's function.

e. *Mapping to Σ and α_{opt}.* In the sub-horizon, quasi-static regime,

$$k^2 (\Phi + \Psi) = -8\pi G a^2 \left[\rho \, \Delta - \underbrace{\left(\tfrac{2\eta}{c_s \ell} + \tfrac{\lambda_1}{\ell^2} + \cdots \right)}_{\kappa_{\text{opt}} \, \rho_{\text{gas}}} \rho_{\text{gas}} \, \underbrace{\ell^2 \sigma_{\mu\nu} \sigma^{\mu\nu}}_{\mathcal{S}_{\text{shock}}} \right] .$$

Thus the local, saturating law $\Sigma = 1 - \alpha_{\text{opt}} \, \mathcal{S}_{\text{shock}}/(1 + \mathcal{S}_{\text{shock}})$ is a compact surrogate for the SK/BRSSS source with $\alpha_{\text{opt}} = \alpha_{\text{opt}}(\eta, \tau_\pi, \lambda_1; T, n_e, B, \ldots)$, $\kappa_{\text{opt}} \sim \frac{2\eta}{\rho_{\text{gas}} c_s \ell} + \frac{\lambda_1}{\rho_{\text{gas}} \ell^2} + \cdots$, rendering α_{opt} *predictive* once transport coefficients are specified. Magnetic fields and collisionality adjust $\eta, \tau_\pi, \lambda_1$ (Braginskii/Spitzer vs. anomalous viscosity), providing additional falsifiers.

f. *Falsifiability.* Given independent inferences of $(\eta, \tau_\pi, \lambda_1)$ from X-ray/radio/shock microphysics, Eq. (**??**) yields a prior on α_{opt}. A persistent mismatch between $\alpha_{\text{opt}}^{\text{SK}}$ and the lensing suppression required to match centroid offsets falsifies the shock-selective channel (Sec. XIII, item (ix)) without touching Parts I–II.

XXV. FROM SK HYDRODYNAMICS TO SHOCK-SELECTIVE Σ: A DERIVATION SKETCH

a. Constitutive input. Starting from the SK generating functional for a near-equilibrium plasma and integrating out UV modes one obtains a causal hydrodynamic EFT with Israel–Stewart/BRSSS constitutive relations. For the traceless anisotropic stress,

$$\pi^{\mu\nu} + \tau_\pi \, \mathcal{D}\pi^{\mu\nu} = 2\eta \, \sigma^{\mu\nu} + \lambda_1 \, \sigma^{\langle\mu}{}_\lambda \, \sigma^{\nu\rangle\lambda} + \mathcal{O}(\nabla^3), \tag{24}$$

where $\eta, \tau_\pi, \lambda_1$ obey Kubo relations (Green–Kubo formulas).

b. Quasi-static, sub-horizon limit. For cluster scales with $\omega\tau_\pi \ll 1$ and $k \gg aH$, the relaxation term is negligible and $\pi^{\mu\nu} \approx 2\eta \, \sigma^{\mu\nu} + \lambda_1 \, \sigma^{\langle\mu}{}_\lambda \sigma^{\nu\rangle\lambda}$. The linearized Einstein equations then yield

$$k^2(\Phi - \Psi) \;=\; 12\pi G a^2 \, \pi^\mu{}_\mu \;\; (= 0 \text{ for traceless}), \tag{25}$$

$$k^2(\Phi + \Psi) \;=\; -8\pi G a^2 \Big[\rho \, \Delta - \underbrace{\kappa_{\rm opt} \, \rho_{\rm gas} \, \ell^2 \, \sigma_{\alpha\beta}\sigma^{\alpha\beta}}_{\text{shock-selective}}\Big] + \cdots, \tag{26}$$

with $\kappa_{\rm opt}$ a positive, dimensionless functional of $(\eta, \tau_\pi, \lambda_1)$ after integrating the quasi-static Green's function.

c. Hubbard–Stratonovich (HS) linearization. The quadratic σ^2 term can be linearized by introducing a traceless auxiliary $Q_{\mu\nu}$,

$$\mathcal{L}_Q = \frac{M^2 m_Q^2}{4} \left(Q_{\mu\nu} - \lambda_Q \, \ell^2 \, \sigma_{\mu\nu}\right)\left(Q^{\mu\nu} - \lambda_Q \, \ell^2 \, \sigma^{\mu\nu}\right), \qquad m_Q^2 \gg H_0^2,$$

so that $Q_{\mu\nu} \simeq \lambda_Q \ell^2 \sigma_{\mu\nu}$ (adiabatic tracking; no new propagating mode) and the lensing source acquires the same local, saturating form as Eq. (**??**) with an amplitude

$$\alpha_{\rm opt} = \alpha_{\rm opt}(\eta, \tau_\pi, \lambda_1; T, n_e, B, \ldots).$$

d. Parametric estimate (order of magnitude). In a shock sheet of thickness $L_{\rm sh}$ with shear rate $|\sigma| \sim \Delta v/L_{\rm sh} \sim \mathcal{M} \, c_s/L_{\rm sh}$, one has $\mathcal{S}_{\rm shock} = \ell^2\sigma^2 \sim (\ell/L_{\rm sh})^2 \mathcal{M}^2$. The effective lensing deficit scales as $\Delta(\Phi + \Psi) \propto \kappa_{\rm opt} \, \rho_{\rm gas} \, \ell^2\sigma^2/k^2$. For ICM values $T \sim (5-15)\,{\rm keV}$ ($c_s \sim 1000\,{\rm km\,s^{-1}}$), $n_e \sim 10^{-3}\,{\rm cm^{-3}}$, $L_{\rm sh} \sim 20-50\,{\rm kpc}$, $\mathcal{M} \sim 2-3$, and moderate effective viscosity (η/s at a few $\times$ Spitzer with magnetic suppression), one finds $\mathcal{S}_{\rm shock} \sim \mathcal{O}(1-5)$ for $\ell \sim 10\,{\rm pc}$ and a dimensionless $\kappa_{\rm opt}$ of order unity, implying a *plausible* $\alpha_{\rm opt} = \mathcal{O}(0.5-1)$ without tuning. A dedicated calibration is left to simulation-aided inference of $(\eta, \tau_\pi, \lambda_1)$.

XXVI. DATA AND CODE AVAILABILITY

Archive DOI (to be finalized before submission): `10.5281/zenodo.TBD`

Reproducible single-file runners:

- `beta_methods_v2.py` (real-space, spectral/Bessel, Euclidean, replica) for β; includes a residual-fitting mode to test for $\ell^4 \log\ell$ contamination in the MI channel; *uses $C_T = 1/(120\pi^2)$ and $(\sigma_1, \sigma_2) = (1/2, 2)$ by default.*

- `cosmology_runner.py` (growth ODE; $\varepsilon_{\rm eff}(a)$ with gates Θ_i; background $\bar{\varepsilon}(a)$ using $f_V^{(i)}$; environment modulation $s(x)$ inside μ).

- `referee_pipeline.py` (FRW averaging module; $\Omega_\Lambda = \beta f c_{\rm geo}$ cross-check with $\bar{\varepsilon}$; computes toy $a_0 = (5/12)\Omega_\Lambda^2 c H_0$).

- `fv_semi_analytic.py` (Press–Schechter/Sheth–Tormen survey for $f_V^{(i)}$; supports a species census with $m_i, \lambda_{\rm mfp}^{(i)}$).

- `gadget4_mu_eps_toy.py` (N-body toy pipeline for growth with $\mu(\varepsilon_{\rm eff}, s)$ and modulation $s(\chi_g)$).

- `s8_hysteresis_run.py` (BAO toy χ_g sweeps; generates `bao_growth.png`).

- `cluster_optics_hook.py` (optional; shock indicator and Σ per Eq. (**??**); two modes: legacy $\alpha_{\rm opt}$ or SK/transport mapping).

- `icm_transport_to_alphaopt.py` (optional; maps $(\eta, \tau_\pi, \lambda_1)$ to $\alpha_{\rm opt}, \kappa_{\rm opt}$).

SYMBOL INDEX

Symbol	Meaning
ℓ	diamond radius (working-order scale)
L_{curv}	local curvature length
$\beta = 2\pi C_T I_{00}$	modular-response sensitivity (QFT coefficient)
C_T	stress-tensor two-point normalization (our convention)
I_{00}	projected ℓ^4 integral coefficient (App. XVI)
$\varepsilon_i,\ w_i$	species i modular state and weight (dof)
$\Theta_i(x;\ell)$	species gate (Eq. 4)
ε_{eff}	species-gated modular state (Eq. 5)
$\bar{\varepsilon}$	$f_V^{(i)}$-weighted background state (Eq. 6)
$\mu(\varepsilon_{\text{eff}}, s)$	growth coupling, $1/(1 + \frac{5}{12}\varepsilon_{\text{eff}} s)$
Σ	lensing coupling (unity on FRW; locally <1 in shocks under D$'$)
$f_V^{(i)}$	species-dependent safe-window volume fraction (App. XX)
$f\, c_{\text{geo}}$	geometric/foliation factor (App. XVII)
κ	local boost surface gravity
β_{KMS}	KMS inverse temperature, $2\pi/\kappa$
T_{KMS}	modular/KMS temperature, $\kappa/(2\pi)$
$s(a)$	modular entropy density proxy, $\sim \beta\, \bar{\varepsilon}(a)\, \ell^{-3}$
χ_g	geometric scalar, $\ell^2 \sqrt{C_{abcd} C^{abcd}}$
$s(\chi_g)$	environment modulation (action-derived envelope)
$\sigma_{\mu\nu}$	baryon shear tensor (symmetric trace-free)
$\mathcal{S}_{\text{shock}}$	shock indicator, $\ell^2 \sigma_{\mu\nu}\sigma^{\mu\nu}$
$Q_{\mu\nu}$	auxiliary traceless tensor (optional, shock-selective optics)
α_{opt}	optical suppression amplitude in Eq. (**??**)
$\eta, \tau_\pi, \lambda_1$	ICM shear viscosity, relaxation time, second-order BRSSS coefficient
κ_{opt}	effective optical coefficient multiplying $\rho_{\text{gas}} \mathcal{S}_{\text{shock}}$
S_8	growth amplitude observable
$\Omega_m(a)$	matter fraction as a function of scale factor
Ω_Λ	dark-energy density parameter

[1] J. J. Bisognano and E. Wichmann, "On the Duality Condition for a Hermitian Scalar Field," *J. Math. Phys.* **16**, 985 (1975); "On the Duality Condition for Quantum Fields," *J. Math. Phys.* **17**, 303 (1976).

[2] H. Casini, M. Huerta, and R. C. Myers, "Towards a derivation of holographic entanglement entropy," *JHEP* **05**, 036 (2011).

[3] H. Osborn and A. C. Petkou "Implications of Conformal Invariance in Field Theories for General Dimensions," *Annals Phys.* **231**, 311–362 (1994).

[4] E. Bellini and I. Sawicki, "Maximal freedom at minimum cost: linear large-scale structure in general modifications of gravity," *JCAP* **07**, 050 (2014).

[5] L. Lombriser and A. Taylor, "Breaking a Dark Degeneracy with Gravitational Waves," *JCAP* **03**, 031 (2016).

[6] T. Jacobson, "Entanglement equilibrium and the Einstein equation," *Phys. Rev. Lett.* **116**, 201101 (2016).

[7] T. Faulkner, A. Lewkowycz, and J. Maldacena, "Quantum corrections to holographic entanglement entropy," *JHEP* **11**, 074 (2013).

[8] N. Lashkari, M. B. McDermott, and M. Van Raamsdonk, "Gravitational Dynamics From Entanglement Thermodynamics," *JHEP* **04**, 195 (2014).

[9] H. Araki, "Relative Entropy of States of von Neumann Algebras," *Publ. Res. Inst. Math. Sci.* **11**, 809–833 (1976).

[10] S. Hollands and R. M. Wald, "Local Wick Polynomials and Time-Ordered-Products of Quantum Fields in Curved Spacetime," *Commun. Math. Phys.* **223**, 289–326 (2001).

[11] C. J. Fewster and S. Hollands, "Quantum Energy Inequalities in Curved Spacetimes," various works.

[12] H. Casini and M. Huerta, "Relative Entropy and Modular Hamiltonians in Quantum Field Theory," various works.

[13] H. Casini, D. A. Galante, and R. C. Myers, "Comments on Jacobson's 'Entanglement equilibrium and the Einstein equation'," *JHEP* **03**, 194 (2016), arXiv:1601.00528.

[14] D. Clowe, M. Bradač, A. H. Gonzalez, M. Markevitch, S. W. Randall, C. Jones, and D. Zaritsky, "A Direct Empirical Proof of the Existence of Dark Matter," *Astrophys. J. Lett.* **648**, L109–L113 (2006).

[15] M. Markevitch, A. H. Gonzalez, L. David, A. Vikhlinin, S. Murray, W. Forman, C. Jones, and W. Tucker, "A Textbook Example of a Bow Shock in the Merging Galaxy Cluster 1E 0657−56," *Astrophys. J. Lett.* **567**, L27–L31 (2002).

[16] R. J. van Weeren, M. de Gasperin, H. Akamatsu, *et al.*, "Diffuse Radio Emission from Galaxy Clusters," *Space Sci. Rev.* **215**, 16 (2019).

[17] A. Mahdavi, H. Hoekstra, A. Babul, D. Balam, and P. Capak, "A Dark Core in Abell 520," *Astrophys. J.* **668**, 806–814 (2007).

[18] W. Israel and J. M. Stewart, "Transient relativistic thermodynamics and kinetic theory," *Annals Phys.* **118**, 341 (1979).

[19] R. Baier, P. Romatschke, D. T. Son, A. O. Starinets, and M. A. Stephanov, "Relativistic viscous hydrodynamics, conformal invariance, and holography," *JHEP* **04**, 100 (2008).

[20] P. Kovtun, "Lectures on hydrodynamic fluctuations in relativistic theories," *J. Phys. A* **45**, 473001 (2012).

[21] L. D. Landau and E. M. Lifshitz, *Fluid Mechanics*, 2nd ed., Pergamon Press (1987).